

**SIMULATION STUDY OF MONOCLONAL ANTIBODY PRODUCTION
USING SUPERPRO; UPSTREAM PROCESS**

MOHD SHAMSUL BIN HUSIN

**A thesis submitted in fulfillment
of the requirements for the award of the degree of
Bachelor of Chemical Engineering (Biotechnology)**

**Faculty of Chemical & Natural Resources Engineering
Universiti Malaysia Pahang**

MAY 2009

I declare that this thesis entitled “Simulation study of monoclonal antibody production using SuperPro; Upstream Process” is the result of my own research except as cited in references. The thesis has not been accepted for any degree and is not concurrently submitted in candidature of any other degree.”

Signature :.....
Name : Mohd Shamsul bin Husin
Date : 2 May 2009

To my beloved parents and teachers

ACKNOWLEDGEMENT

In preparing this thesis, I have been in contact with lecturers, researcher and friends. They have greatly contributed toward completion of this research. I would like to express my gratitude to my supervisor, Miss Nurul Aini binti Mohd Azman for her guidance and support for this report. I would like also to thank Madam Chua@ Yeo Gek Kee for providing data required for my thesis. Not to forget, Muhammad Nur Iman bin Ahmad Razali, my coursemate who conducting similar research for his support.

For abah and mak, your son is grateful for your *hikmah* and *karamah*, I prayed Allah bless your life like how you nuturing me since childhood. I would like also thank my friends especially from PSSCM for their continuous cheering all the way. Abang Dolah, Napi, Ziffi, Mai, Afifah, Pejal, Sheikh, Zulkifli, Zulfadhli and Zulhelmi; I am truly appreciate your moral support and wishing you all the best in the future.

My course mate should also be recognized for their support. My sincere appreciation also extends to all my colleagues and others who have provided assistance at various occasions. Their views and tips are useful indeed. Unfortunately, it is not possible to list all of them in this limited space. I am grateful to all my family members.

ABSTRACT

The purpose of this study is to approximate hybridoma growth kinetic model by comparing simulation result from SuperPro Designer[®] and experimental result. Modeling of hybridoma include calculation of mass for 1 cell and its density. Two kinetic models tested in this study; experimental correlation and de Tremblay *et al.* (1992). Simplification need to be made as this will allow selected model to be used in SPD. Value of μ_{\max} , $K_{S_{GLN}}$, $K_{S_{GLC}}$ are 1.09 d^{-1} (0.05 h^{-1}), 0.3 mM (43.85 mg/L) and 0.1 mM (18.02 mg/L) respectively for de Tremblay and for experimental correlation, their values are 0.158 h^{-1} , 0.0016 mM (0.23 mg/L) and 12.05 mM (2170.93 mg/L) respectively. Experimental data shows no stationary phase but simulation results show stationary phase. From simulation, cell count of 195907.7 while final concentration of glucose, glutamine, ammonia and lactate are 16.38, 4.07, 3.01 and 5.59 mmol/L respectively (experimental correlation) and cell count of 196185.73 while final concentration of glucose, glutamine, ammonia and lactate are 10.73, 2.09, 6.07 and 11.30 mmol/L respectively (de Tremblay). Serious deviations occurred because of simplification on de Tremblay model and inaccurate prediction of glutamine effect on hybridoma's growth. Metabolic reaction used without taking hybridoma real behavior into account. Simulation shows exponential phase without having going through lag phase.

ABSTRAK

Tujuan kajian ini adalah untuk mencari nilai terhampir bagi pemalar penting dalam model kinetik hibridoma dengan menbandingkan keputusan simulasi dari SuperPro Designer[®] dan keputusan eksperimen. Pemodelan hibridoma melibatkan pengiraan jisim satu sel dan ketumpatannya. Dua model kinetik telah diuji di dalam kajian ini; model dari eksperimen dan de Tremblay *et al.* (1992). Terdapat tanggapan perlu dibuat untuk membolehkan model yang dipilih boleh digunapakai bersama SPD. Nilai bagi μ_{\max} , K_{SGLN} , K_{SGLC} are 1.09 d^{-1} (0.05 h^{-1}), 0.3 mM (43.85 mg/L) and 0.1 mM (18.02 mg/L) mengikut urutan bagi de Tremblay dan untuk korrelasi eksperimen, nilainya adalah 0.158 h^{-1} , 0.0016 mM (0.23 mg/L) and 12.05 mM (2170.93 mg/L) mengikut urutan. Data eksperimen menunjukkan tiada fasa statik tetapi data simulasi menunjukkan fasa statik. Dari simulasi, kiraan sel ialah 195907.7 manakala kepekatan akhir glukosa, glutamin, ammonia and laktik adalah 16.38, 4.07, 3.01 and 5.59 mmol/L mengikut urutan (korrelasi eksperimen) dan kiraan sel ialah 196185.73 manakala kepekatan akhir glukosa, glutamin, ammonia and laktik are 10.73, 2.09, 6.07 and 11.30 mmol/L mengikut urutan (de Tremblay). Ralat yang serius berlaku kerana adanya tanggapan terhadap model de Tremblay dan ramalan yang kurang tepat terhadap kesan glutamin kepada pertumbuhan hibridoma. Tindakbalas metabolik dipilih tanpa mengambilkira reaksi sebenar hybridoma terhadap substrak dan hasil metabolik. Fermentasi dalam SPD hanya mengambil kira fasa eksponential.

TABLE OF CONTENTS

CHAPTER	TITLE	PAGE
	DECLARATION	i
	DEDICATION	ii
	ACKNOWLEDGEMENTS	iii
	ABSTRACT	iv
	ABSTRAK	v
	TABLE OF CONTENTS	vi
	LIST OF SYMBOLS	viii
	LIST OF FIGURES	xi
	LIST OF TABLES	x
1	INTRODUCTION	1
	1.1 Background of Study	1
	1.2 Problem Statement	3
	1.3 Objectives	4
	1.4 Scope of Study	4
	1.5 Rationale and Significance	4
2	LITERATURE REVIEW	5
	2.1 Dynamic Modeling and Simulation	5
	2.2 Scale-up and Optimization	11
	2.2.1 Stirred tank bioreactor	11
	2.2.2 Optimization	14

3	METHODOLOGY	15
	3.1 Stoichiometric Expression and Kinetic Parameters	15
	3.2 Simulation and data comparison	15
4	RESULT AND DISCUSSION	19
	4.1 Modelling of hybridoma	19
	4.2 Raw experimental data	20
	4.3 Linearized Monod Equation	22
	4.4 de Tremblay <i>et al.</i> (1992)	24
	4.5 Comparison between experimental and simulation result	26
5	CONCLUSION AND RECOMMENDATION	27
	5.1 Conclusion	27
	5.2 Recommendation	28
	REFERENCES	29

LIST OF SYMBOLS

[AMM]	-	Ammonia concentration
[GLC], S1	-	Glucose concentration
[GLN], S2	-	Glutamine concentration
[LAC]	-	Lactate concentration
B-Term	-	Biomass concentration
K_s	-	Half-saturation constant
k_d	-	Specific death rate
S1-Term, S2-Term	-	Monod equation
M_1, M_2, M_3	-	Reaction intermediates
MAB	-	Monoclonal antibody
P_g/V	-	Power input per volume
X	-	Cell density
α	-	Empirical constant
μ	-	Specific growth rate
μ_{max}	-	Maximum specific growth rate
β	-	Death constant

LIST OF FIGURES

FIGURE NO.	TITLE	PAGE
1.1.1	Development of monoclonal antibody from 1975 until 2002 (A.C.A Roque <i>et al.</i> , 2004)	2
2.1.1	Model system of mammalian cell that include glucose (S1), glutamine (S2), cell density (X) and enzyme (e_i) (Maria J.G <i>et al.</i> , 2000)	7
2.1.2	Metabolic network of hybridoma (J. Gao <i>et al.</i> , 2007)	7
2.2.1.1	Influence of impeller and power input on formation of bubbles (M. Martin <i>et al.</i> , 2008, Part 1)	13
2.2.2.1	Optimization of fed-batch bioreactor operation (C. Kontoravdi <i>et al.</i> , 2007)	14
4.2.1	Concentration of substrate and metabolite versus time (raw data)	19
4.2.2	Viable cells count versus time (raw data)	20
4.3.1	$1/\mu$ versus $1/s$	21
4.3.2	Concentration of substrate and metabolite versus time (linearized Monod equation)	22
4.3.3	Viable cells count versus time (linearized Monod equation)	22
4.4.1	Concentration of substrate and metabolite versus time (de Tremblay)	24
4.4.2	Viable cells count versus time (de Tremblay)	24

LIST OF TABLES

TABLE NO.	TITLE	PAGE
2.1.1	Kinetic Parameter Obtained (L.Legazpi <i>et al.</i> , 2005)	6
2.1.2	Fundamental macro reaction of mammalian cell culture (J. Gao <i>et al.</i> , 2007)	8
2.1.3	Catabolic reaction with condition simplification (Y.H. Guan and R.B. Kemp, 1999)	9
2.1.4	Various correlations of kinetic parameters (R. Pörtner and T. Schäfer, 1996)	11
2.2.1.1	Geometric details of stirred tank bioreactor (B.N. Murthy <i>et al.</i> 2007)	13
3.2.1	Parameter and initial condition of T-flask	17
3.2.2	Hybridoma growth profile	18

CHAPTER 1

INTRODUCTION

1.1 Background of Study

Monoclonal antibody (MAb) is an antibody of single type, i.e. will bind only to one antigen. It is favored as pharmaceutical product because it can be administered at high dosage because of low potency. A.C.A Roque *et al.* (2004) has classified MAbs into three types. The first type is chimeric Mab, developed by joining DNA segment of mouse encoding variable region with human constant region. Second type is transgenic MAb, obtained from genetically engineered animals and third type is recombinant antibody fragment, traditionally obtained by partial digestion of immunoglobulin with proteases. Antigen detected including botulinum toxin, that cause muscular paralysis produced by *Clostridium botulinum*, been considered as bioterrorism agent (L.H Stanker *et al.*, 2008) and infection by B19 parvovirus that may cause paralysis and spontaneous abortion to pregnant women (M.D. Drechsler *et al.*, 2008). Other application of MAb is in chromatographic separations to purify protein molecules.

Hybridomas, hybrid between myeloma and B-lymphocytes developed in 1970s capable of the continuous production of monoclonal antibodies (M. Butler, 2004). Myeloma is cancerous cell which readily cultivated and have infinite lifespan while B-lymphocytes able to synthesis single antibody (Prescott *et al.* 2005). Up until 2004, more than two dozen antibody-based products commercially available.

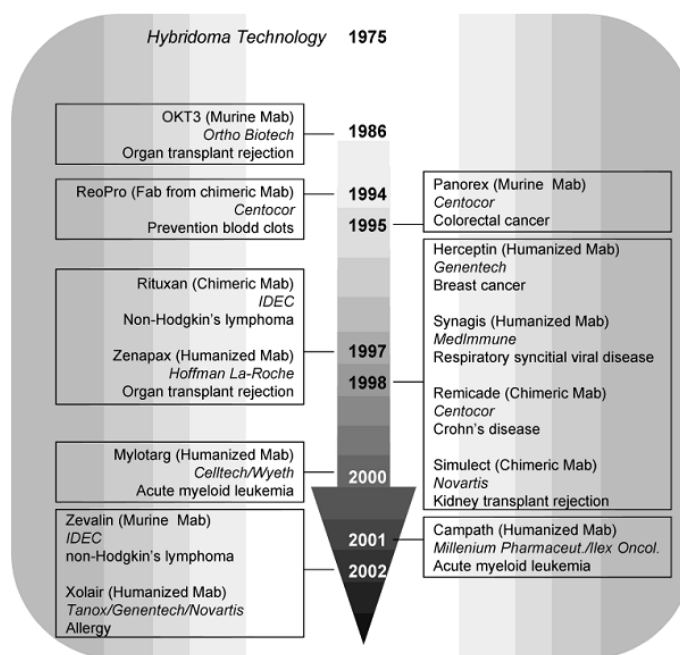


Figure 1.1.1: Development of monoclonal antibody from 1975 until 2002
(A.C.A. Roque *et al.*, 2004)

Upstream process involved cell line development, media optimization and cell culture optimization (Feng Li, Joe X. Zhou *et al.* 2005). Upstream process has improved 100 folds for the last 15 years resulted from improvement in expression technology and process optimization (J.R. Birch, A.J. Racher, 2006), especially feeding strategies. Scaling-up antibody manufacturing process usually has mixed opinion, either increase size or increase number of reactor because chemical process parameter is not very reliable in scaling up biological process.

This question is solved by using integrated flow sheet and process simulation. SuperPro Designer[®] (SPD) developed by Intelligen Inc. is suitable software for providing computing environment because it more on bioprocess operation compared to Aspen BPS[™] which focused on chemical process (S.A. Rouf *et al.* 2001). Application of computer aided simulation has been slow in biopharmaceutical industries but it has gained popularity. It able to reduces time and cost on building pilot-scale plant. Simplicity and fast setup are key advantages in using SPD but, user unable to build customized model (S.S Farid *et al.*,2007).

1.2 Problem Statement

Cost of producing MAb at large scale is extremely high. S.S Farid (2006) reported \$660 to \$1580/ft² and \$1756 to \$4220/L invested on antibody manufacturing site with total site capacities of 2000 L to 20000 L. This investment does not account for miscellaneous cost such as clinical testing, validation and approval of the product.

Literatures [L.H. Stanker *et al.*, 2008, M.D Drechsler *et al.*, 2008] have shows slowest step in upstream process is cell line development where it can take 14 to 30 days to develop. Mammalian expression system such as mouse myeloma (NS0) and Chinese hamster ovary is the most effective way in generating MAb, yet it is very costly (A.C.A Roque *et al.*, 2004) while *molecular pharming* (extracting MAb directly from transgenic animals and plant) has shown no clinical result even though it has lower capital cost.

Expression error is also common problems in MAb production such as error in glycosylation (C. Kontoravdi *et al.* 2007) allowing degradation of processed antibody and increased sensitivity of genetically modified cells to the surrounding (E. Jain, A. Kumar, 2008). Obstacles encountered in scaling up are where parameter optimization such as pH, temperature, agitation rate, oxygen supply control that been ignored at bench scale (less than 5 L of culture). Limited data on growth rate also another problem, causing optimization based on trial-and-error. Shuler and Kargi (2002) write; in larger scale, it is difficult to maintain homogeneity and change in culture itself due to increase time of culture.

1.3 Objectives

1.3.1 To approximate hybridoma viable cell growth rate by comparing simulation data and real-time data on bench-scale fermentation.

1.4 Scope of Study

Model for this study is hybridoma used to cultivate antibody towards C-cell hyperplasmic (CCH), an inherent disease, which able to cause death to month year old infant, paralysis and sexual deficiency. Simulation of this process limited to hybridoma's unstructured model of cell metabolism towards glucose and glutamine. Simulation is conduct by assuming no external disturbance. Material and energy balance

done by using unstructured growth model i.e. balance around fermenter and all parameter tested limited to the features provided by SuperPro[®] Designer 6.0 build 11.

1.5 Rationale and Significance

This study has potential in minimizing economical losses by replicating sensitivity of cell and properties of media into integrated flow sheet, aiding analysis on proposed change in MAb's production by predicting the results before process scaling-down to ensure its feasibility. Rate equation gained from this study approximate real-time data; it will decrease number of bench-scale experiments require to investigate essential parameters for large-scale operation.

CHAPTER 2

LITERATURE REVIEW

2.1 Dynamic Modeling and Simulation

Main source of nutrients for mammalian cell culture are glucose and glutamine. Metabolism of both substrates is related via TCA cycle (Maria J.G *et al.* 2000). Research strategy proposed by C. Kontoravdi *et al.* 2004 are proposing mathematical model for growth, gathering experimental data and use it to validate the model, build a robust model to explain the growth; in sequence. C. Kontoravdi *et al.* 2007 by modeling specific cell growth rate based on concentration of substrates (glutamine and glucose) and metabolites (ammonia and lactate). Typical modeling of hybridoma metabolism involved glutamine and glucose as elementary reaction for simplification, making it feasible for optimization process. Another view (R. Pörtner and T. Schäfer, 1996) says modeling on those two components because of ease of analysis. Assumption made when deriving dynamic model for inoculums are cells grow exponentially, isothermal operation, liquid density is constant, treating solid (biomass) and liquid as homogenous (Seborg, 2004). Simplification is made by using unstructured growth model for computational tractability. Assumptions made in solving this equation are specific growth rates and consumption rates were constant during exponential phase (L.Legazpi *et al.* 2005) as described in Table 2.1.1. S.S. Ozturk *et al.* (1991) reported meaningful kinetic parameter can be obtained in absence of lag phase and meticulous selection on time span of exponential phase.

	Bree et al. [3]	Jeong and Wang [7]	Miller et al. [8]	Harigae et al. [11]	Ozturk and Palsson [22]	This work
Medium	DMEM	DMEM	DMEM	ERDF + growth factors	IMDM	Hybrimax
% FBS	5	5	10	0	5	0
Cell line	SP2/0	V111 H-8	AB2-143.2	NS1	167.4G5.3	HB-8852
μ_{app} (h ⁻¹)						0.014
k_d (h ⁻¹)					0.004	0.0046
μ (h ⁻¹)	0.125	0.033	0.063	0.022–0.044	0.042	0.019
p_{Lac} (μmol cell ⁻¹ h ⁻¹)					3.8×10^{-7}	7.5×10^{-7}
p_{Am} (μmol cell ⁻¹ h ⁻¹)					3.1×10^{-8}	6.9×10^{-8}
p_{MAb} (pg cell ⁻¹ h ⁻¹)					0.22	2.1
q_{Glc} (μmol cell ⁻¹ h ⁻¹)					2.2×10^{-7}	4.6×10^{-7}
q_{Gln} (μmol cell ⁻¹ h ⁻¹)					4.6×10^{-8}	1.1×10^{-7}
$Y_{Lac/Glc}$			1.3–2.1		1.8	1.6
$Y_{Am/Gln}$			0.34–0.66		0.58	0.63

Table 2.1.1: Kinetic parameters obtained (L. Legazpi *et al.*, 2005)

$$\mu = \mu_{max} f_{lim} f_{inh},$$

$$f_{lim} = \left(\frac{[GLC]}{K_{glc} + [GLC]} \right) \left(\frac{[GLN]}{K_{gln} + [GLN]} \right),$$

$$f_{inh} = \left(\frac{KI_{lac}}{KI_{lac} + [LAC]} \right) \left(\frac{KI_{amm}}{KI_{amm} + [AMM]} \right),$$

Equation 2.1.1: Unstructured model of growth (C. Kontoravdi *et al.* 2007)

$$r_j = [\alpha \mu_{max} (S1 - Term)(S2 - Term) + \beta] (B - Term)$$

Equation 2.1.2: Rate of growth applied in SPD

This is necessary to create model based on stoichiometry that is useful for studying relative activity of pathways under various culture conditions. However, this model unable to explain regulation and control of cellular activity which only be described by less available dynamic model (J. Gao *et al.* 2007). Dynamic model as explained by D.B.F. Faraday *et al.* 2001 employs genetic control over cell cycle regulation. C. S Sanderson *et al.* 1999 reported dynamic model require manual tuning since available automatic estimation routines is limited. S.S. Farid (2006) view dynamic model from economy as tool relating time –dependent operation with discrete simulation techniques that provide more realistic schedule. Prediction is relatively poor and J. Gao *et al.* 2007 conclude identification of reaction kinetics is crucial because of nonlinearity and over-parametrization of model. C.S Sanderson *et al.* 1999 reported too, modeled cell has no stationary phase and some data shows linearity with the model. The main difficulty in

modeling hybridoma cell is lacks of literature but, parameters from Chinese Hamster Ovary (CHO) applicable as CHO cells also produce and glycosylate MAbs.

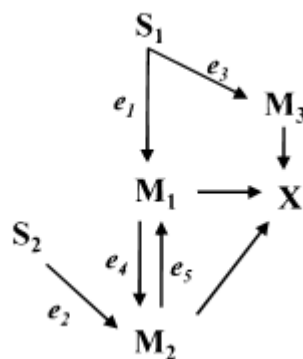


Figure 2.1.1: Model system of mammalian cell that include glucose (S1), glutamine (S2), cell density (X) and enzyme (e_i) (Maria J.G. *et al.* 2000)

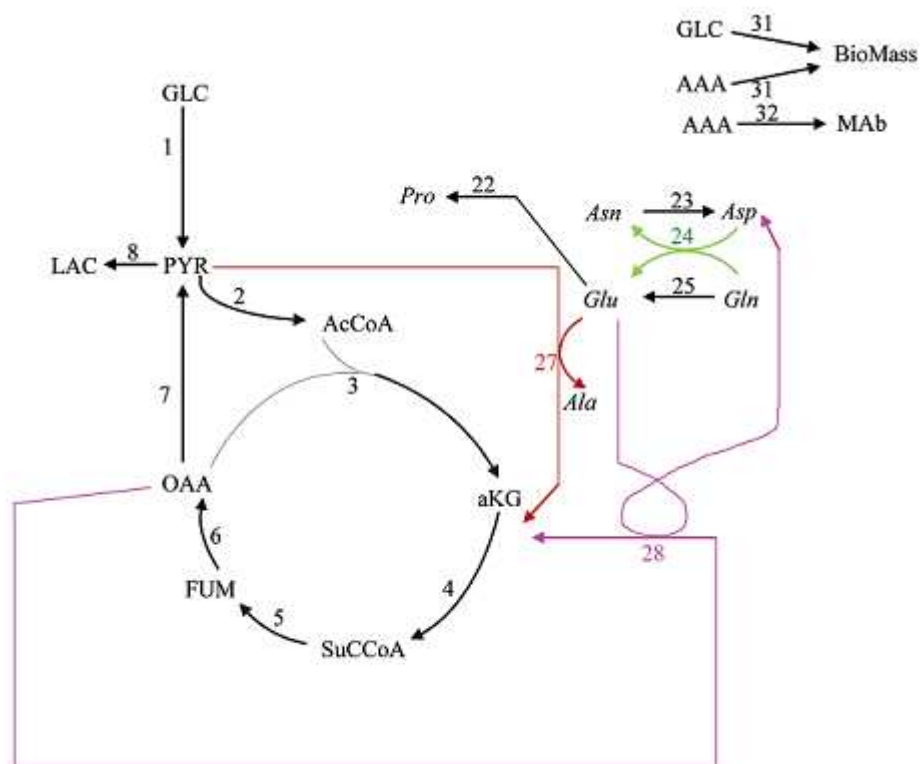
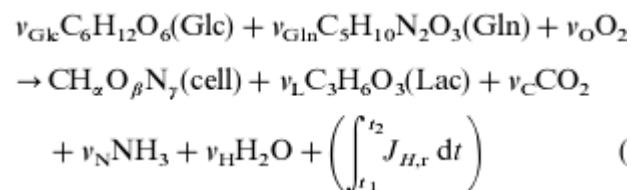


Figure 2.1.2: Metabolic network of hybridoma (J.Gao *et al.* 2007)

E1	GLC → 2LAC
E2	GLC + 2GLU → 2Ala + 2CO ₂ + 2LAC
E3	GLC + 2GLU → 2Asp + 2LAC + 6CO ₂
E4	GLU → PRO
E5	ASN → ASP + NH ₃
E6	GLN + ASP → ASN + GLU
E7	0.0508GLC + 0.0577GLN + 0.0133ALA + 0.007ARG + 0.006ASN + 0.0201ASP + 0.0004CYS + 0.0016GLU + 0.0165GLY + 0.0033HIS + 0.0084ILE + 0.0133LEU + 0.0101LYS + 0.0033MET + 0.0055PHE + 0.0081PRO + 0.0099SER + 0.008THR + 0.004TYR + 0.0096VAL → BioMass
E8	0.0104GLN + 0.011ALA + 0.005ARG + 0.0072ASN + 0.0082ASP + 0.005CYS + 0.0107GLU + 0.0145GLY + 0.0035HIS + 0.005ILE + 0.0142LEU + 0.0145LYS + 0.0028MET + 0.0072PHE + 0.0148PRO + 0.0267SER + 0.0160THR + 0.0085TYR + 0.0189VAL → MAb
E9	GLN → GLU + NH ₃

Table 2.1.2: Fundamental macro reaction of mammalian cell culture (J. Gao *et al.* 2007)

Figure 2.1.1, Figure 2.1.2 and Table 2.1.2 shown above are consistent with finding by D.B.F Faraday suggesting glutamine as source of energy and glucose as source of biomass. This statement agreed with S.S Ozturk *et al* (1991) stating glutamine as major source of energy and growth ceased when it depleted. There is contradiction between D.B.F Faraday *et al.* (2001) and J. Gao *et al.* (2007) where Faraday assume glutamine consumption to be in zero-order and glucose consumption in first-order while J. Gao using Monod kinetics in his research. H.Znad *et al.* (2004) explained kinetic parameters such as oxygen transfer are scale-dependent. Maria J.G *et al.* (2000) modeling is consistent with modeling by Y.H. Guan and R.B. Kemp (1999) by omitting micronutrients and minor catabolites that does not have effect on enthalpy recovery as shown in Equation 2.1.3 and Table 2.1.3.



Equation 2.1.3: Growth reaction (Y.H. Guan, R.B. Kemp, 1999)

Metabolic condition	Condition simplification	Catabolic reaction	Enthalpy recovery ($J_0/J_{H1} \times 100$) (%)
Activated cells	Lactate only	$C_6H_{12}O_6 + 0.3466C_3H_{10}N_2O_3 + 1.7956O_2$ $\rightarrow 1.9213C_3H_6O_3 + 1.9689CO_2 + 0.6931NH_3 + 0.9292H_2O$	92.9
	Lactate + pyruvate	$C_6H_{12}O_6 + 0.338C_3H_{10}N_2O_3 + 1.750O_2$ $\rightarrow 1.873C_3H_6O_3 + 0.0613C_3H_4O_3 + 1.888CO_2 + 0.676NH_3 + 0.936H_2O$	93.5
	Lactate + glutamate	$C_6H_{12}O_6 + 0.420C_3H_{10}N_2O_3 + 1.710O_2$ $\rightarrow 1.830C_3H_6O_3 + 0.180C_3H_9NO_4 + 1.830CO_2 + 0.660NH_3 + 0.812H_2O$	93.1
Triggered cells	Lactate only	$C_6H_{12}O_6 + 0.3167C_3H_{10}N_2O_3 + 3.8359O_2$ $\rightarrow 1.1964C_3H_6O_3 + 3.9942CO_2 + 0.6333NH_3 + 3.044H_2O$	94.7
	Lactate + pyruvate	$C_6H_{12}O_6 + 0.291C_3H_{10}N_2O_3 + 3.525O_2$ $\rightarrow 1.10C_3H_6O_3 + 0.194C_3H_4O_3 + 3.573CO_2 + 0.582NH_3 + 2.894H_2O$	95.0
	Lactate + glutamate	$C_6H_{12}O_6 + 0.380C_3H_{10}N_2O_3 + 3.598O_2$ $\rightarrow 1.123C_3H_6O_3 + 0.165C_3H_9NO_4 + 3.704CO_2 + 0.594NH_3 + 2.896H_2O$	94.5

Table 2.1.3: Catabolic reaction with condition simplification (Y.H. Guan and R.B. Kemp, 1999)

This will determine environment of bioreactor as time length of culture have change (Shuler and Kargi, 2002). Cell death can occurred in two ways, apoptosis (programmed cell death under genetic control) and necrosis (disintegration of cell by external stress); both caused by substrate limitation and metabolite inhibition, respectively (R. Pörtner and T. Schäfer, 1996) as illustrated in Table 2.1.4.

Reference	Specific growth rate μ	Specific death rate μ_d
de Tremblay et al. (1992)	$\mu_{\max} \frac{Glc}{K_{Glc} + Glc} \frac{Gln}{K_{Gln} + Gln}$	$\frac{K_{d,\max}}{(\mu_{\max} - K_{d,Lac})(\mu_{\max} - K_{d,Amm} Amm)} \times \frac{K_{d,Gln}}{K_{d,Gln} + Gln}$
Frame and Hu (1991a)	$\mu_{\min} + \frac{(\mu_{\max} - \mu_{\min})(Glc - Glc_{th})}{K_{Glc} + (Glc - Glc_{th})}$	$(\mu_{\min} - D_{\min}) - \frac{K_{d,\max}(Glc - Glc_{th})}{K_d + (Glc - Glc_{th})}$
Bree et al. (1988)	$\mu_{\max} \frac{Gln}{K_{Gln} + Gln} \frac{K_{Amm}}{K_{Amm} + Amm} \frac{K_{Lac}}{K_{Lac} + Lac}$	$K_d \cdot \frac{Amm}{K_{d,Amm} + Amm} \cdot \frac{Lac}{K_{d,Lac} + Lac} \cdot \frac{K_{d,Gln}}{K_{d,Gln} + Gln}$
Kurokawa et al. (1994)	$\mu_{\max} \frac{Glc}{K_{Glc} + Glc} \frac{K_{Lac}}{K_{Lac} + Lac}$	—
Miller et al. (1988)	$\mu_{\max} \frac{Glc}{K_{Glc} + Glc} \frac{Gln}{K_{Gln} + Gln} \times \frac{K_{Amm}}{K_{Amm} + Amm} \frac{K_{Lac}}{K_{Lac} + Lac}$	—
Dalili et al. (1990)	$\mu_{\max}(Ser_i) \frac{Gln}{K_{Gln} + Gln}$	$K_{d,\min} + (K_{d,\max} - K_{d,\min}) \frac{K_d}{K_d + Gln}$
Linardos et al. (1991)	$D + d_0 e^{-\mu}$	$d_0 e^{-\mu}$
Batt and Kompalla (1989)	As a function of intracellular constituent pools	$K_d \frac{Amm}{K_{d,Amm} + Amm} \frac{Lac}{K_{d,Lac} + Lac}$
Gaertner and Dhurjati (1993)	$0.043 \frac{B - 0.07}{B}$	—
Glacken et al. (1989)	$\frac{\mu_{\max} Ser Gln}{[Ser + (K_{s,0} X^{-\beta})(K_{Gln} + Gln)(1 + \frac{Amm^2}{K_{Amm}})]}$	$0.051 e^{-101.2 \cdot \mu}$
Pörtner et al. (1996)	$\mu_{\max} \frac{Gln}{Gln + K_{Gln}}$	$0.002 + \frac{6 \times 10^{-5}}{Gln + 0.0025}$

Reference	μ_{\max} (h ⁻¹)	K_{Glc} (mM)	K_{Gln} (mM)	Medium	Glc (mM)	Gln (mM)
de Tremblay et al. (1992)	0.045	1	0.3	DMEM, 10% FCS	25	4
Frame and Hu (1991a)	0.063	0.034	—	DMEM-L, 10% FCS	5.56	4
Bree et al. (1988)	0.125	—	0.8	DMEM, 5% FCS	25	4
Kurokawa et al. (1994)	0.033	0.28	—	RDF, serum-free	Var.	Var.
Miller et al. (1988)	0.063	0.15	0.15	DMEM, 10% FCS	22	4.8
Dalili et al. (1990)	0.056	—	0.06	RPMI, 20% FCS	13.8	1.5
Linardos et al. (1991)	~0.04	—	—	DMEM, 1.5% FBS	25	4.8
Gaertner and Dhurjati (1993)	0.043	—	—	DMEM, 10% FCS	Var.	Var.
Glacken et al. (1989)	0.055	—	0.15	DMEM, 0.75-1% FCS	25	4
Pörtner et al. (1996)	0.036	—	0.06	IMDM/Ham's F12, 3% HS/ FCS	17.5	4

Reference	Correlation	Substrate	$Y_{X,S}$ (10^8 cells mmol^{-1})	m (10^{-10} mmol^{-1} cell $^{-1}$ h $^{-1}$)
Miller et al. (1988)		Glc	2.80	0.50
Harigae et al. (1994)	$\frac{\mu}{Y_{X,S}} + m$	Glc	5.88	0.51
		Gln	3.44	0.08
Hiller et al. (1991)		Glc	1.02	—
		Gln	16.9	1.56
Linardos et al. (1991)	$\frac{\mu}{Y_{X,S}} + m - e \cdot \mu_D$	Glc	5.93	1.96
		Gln	6.30	0.29
Frame and Hu (1991b)	$\frac{\mu}{\frac{1}{Y_{X,S}} + \frac{\beta}{Y_{P,S}} + \frac{\alpha}{Y_{P,S}} \frac{\mu_{\min}}{Y_{X,S}}}$	Glc	"	—
de Tremblay et al. (1992)	$\frac{\mu}{Y_{X,S}}$	Gln	3.80	—

Table 2.1.4: Various correlations of kinetic parameters (R. Pörtner and T. Schäfer, 1996)

2.2 Scale-up and Optimization

Bioreactor should be designed to provide both low shear to cells and adequate mass transfer between nutrient or waste and cells to achieve high cell density (E. Jain and A. Kumar, 2008). B.N Murthy et al. (2007) emphasis performance of reactor involving suspended solid greatly influences by dispersion of gas and solid particles as reaction occurred between dissolved gas and solid with liquid as inert. Scale-up by using geometric similarity require equality in agitation power per volume, volumetric oxygen mass transfer coefficient, maximum shear stress and mixing time (Solá and Gódia, 1995). Heat transfer equipment among equipment facing difficulties in scale-up

2.2.1 Stirred tank bioreactor

Shuler and Kargi (2002) and E. Jain and A. Kumar (2008) agreed reactor with internal agitation suitable for commercial purpose because of flexibility and high mass transfer coefficient. Flexibility come from ease of changing mechanical part especially impeller; position and rotation speed of impeller influence mass transfer coefficient by adjusting height of impeller.

At higher position or low rotational speed, impeller virtually has no effect on bubbles deformation as bubbles may avoid impeller (M. Martin et al., 2008, part 1). Figure below shows influence on bubbles' formation time by type of impeller and power input. Ruston turbine has been considered most stable because surface

aeration increase with position of the impeller and bubbles break up due developed flow under the impeller (M. Martin *et al.*, 2008, part 2) as shown in Figure 2.2.1.1. For power input less than 0.1 W/kg, the mass transfer rate is given by the rising bubbles from non-stirred fluid. From 0.1 to 1 W/kg, stirring is not crucial in mass transfer mechanism and mass transfer rate increase with dissipated energy yet, remain stable. Simulation using FLUENT 6.25 run by B.N Murthy *et al.* (2007) on three impeller designs as shown in Table 2.2.1.1 shows amount of settling solid in a reactor decrease as rotational speed increase but it have small effect near the surface of liquid. Each design develops unique flow pattern meaning different efficiency because flow pattern is essential in deforming bubbles.

Another factor influence efficiency of fermenter is gas flow rate. At larger gas flow rate, time taken for bubbles formation decreased slightly (M.Martin *et al.*, 2008, Part 1). Reduces in solid's cloud height observed by B.N. Murthy *et al.* (2007) as solid settle down when superficial gas velocity decreased. Comparing two-holes and one-holes sparger, two-holes sparger require less energy input since bubbles formed is small and has large contact area, improving mass transfer. Chisti (1993) explain scale-up based on bulk flow have advantage in keeping aeration rate low because breakup of bubbles in not necessary. Particle size also have important role in determining critical speed of impeller because at smaller size, it has high homogeneity with medium, thus less energy required to suspend the solid.

Reactor geometry	Impeller	Solids details	Operating variables
$T = 0.39$ m, $H = 1.19T$, $C = T/3$	4-PBTD, $D = T/3$	Glass particles: $\rho_S = 2660$ kg/m ³ , $d_p = 0.15, 0.225, 0.45$ mm	Solid conc. = 0.5 kg/100 kg, $N = N_{js}$
$T = 0.50$ m, $H = T$, $C = T/3$	6-PBTD, $D = T/3$		$N = 210$ rpm, ring sparger = 0.116, sparger location = 0.1 m $V_G = 0.151$ /s
$T = 0.19$ m, $H = T$, $C = T/3$	6-PBTD, $D = T/2$		$N = 300$ rpm, ring sparger = 0.8D, sparger location = 0.6C, $V_G = 0.0421$ /s
$T = 0.20$ m, $H = T$, $C = T/3$	4-PBTD, $D = T/3$	Glass particles: $\rho_S = 2520$ kg/m ³ , $d_p = 327$ μ m	Solid conc. = 1, 2, 3 vol%, $N = 1000$ rpm

Table 2.2.1.1: Geometric details of stirred tank reactor (B.N. Murthy *et al.* 2007)

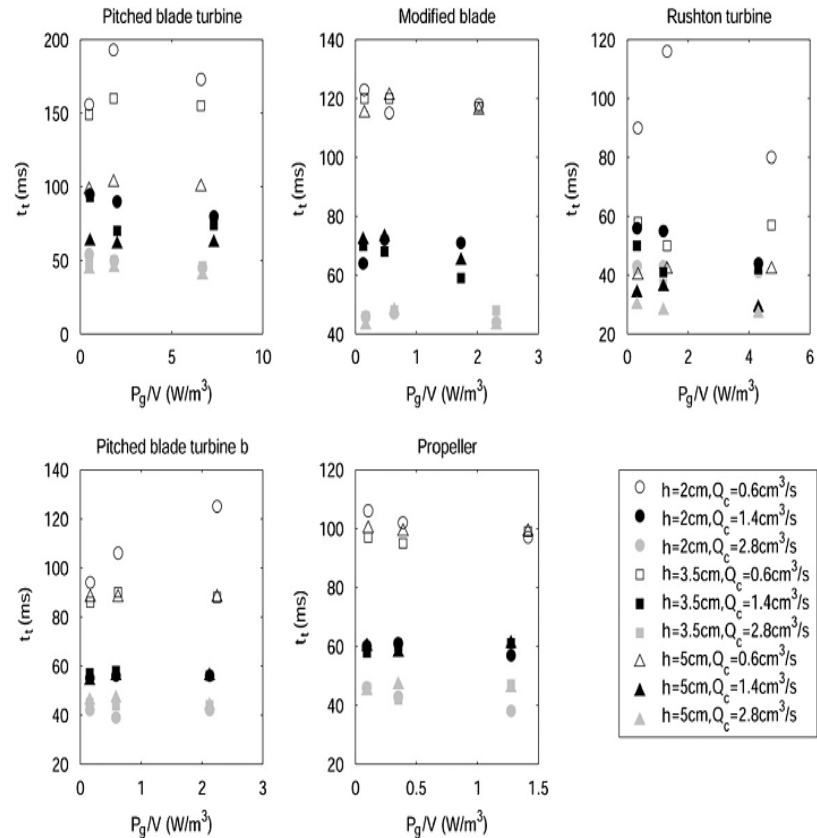


Figure 2.2.1.1: Influence of impeller and power input on formation time of bubbles (M.Martin *et al.* 2008, Part 1)

Axial flow hydrofoil agitator is used to disperse gas (E. Jain and A. Kumar, 2008) because it has lower energy demand and reduced maximum shear rate (Shuler and Kargi, 2002). Comparing finding on aeration and agitation effect by Chisti (1993) with review by E.Jain and A.Kumar (2008), hybridoma can withstand high shear rate in reactor volume up to 0.3 m^3 . Hybridoma cells able to withstand turbulence flow regime in bioreactor.

2.2.2 Optimization

Fed-batch process most common in production of MAb (J.R Birch and A.J Racher, 2006) and analysis using Monte Carlo simulation shows fed-batch has higher reward/risk ratio compared to cell perfusion system (S.S Farid, 2006). Optimization of feed based on trial-and-error iteration on addition and depletion of nutrients [J.R Birch and A.J Racher, 2006; E. Jain and A. Kumar, 2008]. Optimization result as shown in Figure 2.2.2.1. Inhibition effect by ammonia and